Simulation of Wave Propagation in Media Described by Fractional-Order Models

Tomasz P. Stefański
Faculty of Electronics, Telecommunications, and Informatics
Gdansk University of Technology
Gdansk, Poland
tomasz.stefanski@pg.edu.pl

Jacek Gulgowski
Faculty of Mathematics, Physics and Informatics
University of Gdansk
Gdansk, Poland
jacek.gulgowski@mat.ug.edu.pl

Abstract—In this paper, algorithms for simulation of the wave propagation in electromagnetic media described by fractional-order (FO) models (FOMs) are presented. Initially, fractional calculus and FO Maxwell's equations are introduced. The problem of the wave propagation is formulated for media described by FOMs. Then, algorithms for simulation of the non-monochromatic wave propagation are presented which employ computations in the time domain (TD) and the frequency domain (FD). In the TD algorithm, the electromagnetic field is computed as a convolution of an excitation with Green's function formulated based on an improper integral and the Mittag-Leffler function. On the other hand, the FD algorithm transforms an analytic excitation to FD, executes multiplications with phase factors, and finally transfers back result to TD. This algorithm involves elementary functions only, hence, computations are significantly faster and accurate with its use. However, applicability of the FD algorithm is limited by the sampling theorem. Numerical results and computation times obtained with the use of both algorithms are presented and discussed in detail.

Index Terms—Computational electromagnetics, electromagnetic propagation, Maxwell's equations, fractional calculus.

I. INTRODUCTION

In 1889, Jacques Curie formulated an experimental law describing the current $i(t)$ through a capacitor under the voltage excitation $v(t)$ being the Heaviside step function [1]. An application of the constant dc voltage U_0 to a dielectric material between electrodes at the time $t = 0$ results in a current given by $i(t) = U_0/(h_1 t^\beta)$, where $\beta \in (0,1)$ is related to losses and h_1 is related to the capacitance of such a capacitor. Hence, the measured response of a capacitor is significantly different from predictions of the classical circuit theory and cannot be understood in terms of the standard theory of capacitance. Currently, this experimental result is known as Curie's law. In 1994, Westerlund and Ekstam announced [2] that they altogether had measured tens of thousands of various capacitors and had never experienced a capacitor that does not closely adhere to Curie's law. Hence, they proposed the relationship between the voltage and the current of the capacitor in the form $i(t) = C_\beta D_t^\beta v(t)$, where C_β denotes the pseudo-capacitance and D_t^β denotes the fractional-order (FO) derivative. In this model, the standard relation between the current and the voltage drop at the capacitor is obtained when $\beta = 1$. Thus, it means that FO modelling does not replace the standard circuit theory but only extends it.

Recently, with the use of FO derivatives [3], [4], the mathematical modelling of a skin effect has been proposed which extends standard circuit models of inductive elements. Furthermore, FO Maxwell's equations have been formulated [5]–[9], which allow for inclusion of the skin effect as well as memory effects of material polarization and magnetization in electromagnetic models. Such FO Maxwell's equations can be useful for describing the evolution of electromagnetic systems with memory which are dissipative and very complex.

FO electromagnetic systems are also investigated in microwave engineering. FO models (FOMs) of lumped elements are developed [10], [11]. The FO modelling of electromagnetic waveguiding is investigated in hollow waveguides [12] and transmission lines [13], [14]. Furthermore, the classical method of microwave circuit analysis based on the Smith chart is extended towards FO modelling [15]. In [16], [17], a causal and compact FO transmission line model for THz frequencies is developed for CMOS on-chip conductor. For this model, a good agreement of the characteristic impedance is observed with measurements up to 110 GHz. However, the traditional integer-order (IO) model agrees with measurements only up to 10 GHz. These results clearly demonstrate advantages of the transmission line modelling based on FO derivatives.

Investigations of possible novel effects and phenomena observed when the FO time-derivatives are enabled in Maxwell's equations are currently needed. It stems from the fact that such research can stimulate future applications of FO electromagnetic systems. Hence, we have recently developed the algorithms for simulation of the non-monochromatic wave propagation in the time domain (TD) and the frequency domain (FD) [18], [19], which allow one to investigate the general properties of electromagnetic waves in media described by FOM (i.e., so called diffusive waves). In this contribution, both algorithms are compared in terms of accuracy and computation times. In the TD algorithm, the electromagnetic field is computed as a convolution of an excitation with TD Green's function formulated based on an improper integral and the Mittag-Leffler function. On the other hand, the FD algorithm transforms an analytic excitation to FD, executes multiplications with phase factors, and finally transfers back result to TD. This algorithm involves elementary functions only, hence, its computation time is significantly smaller

than for the TD algorithm. However, applicability of the FD algorithm is limited by the sampling theorem [20]. Numerical results obtained with the use of both algorithms are presented and discussed in detail. Our results favour the FD method in terms of accuracy and computation times.

II. FRACTIONAL CALCULUS

In the presented below formulation of the FO electromagnetic theory, the *Marchaud derivative* concept is applied (refer to Sections 5.4 and 5.6 in [21] and Section 1.3.1 in [22] as well as refer to [23] for a historical discussion). The Marchaud derivative of the order $\alpha \in (n-1, n)$, $n \in \mathbb{N}$ is defined as

$$
\begin{aligned}
D^\alpha f(t) &= \\
&= \frac{\{\alpha\}}{\Gamma(1-\{\alpha\})} \int_0^{+\infty} \frac{f^{(n-1)}(t) - f^{(n-1)}(t-\tau)}{\tau^{1+\{\alpha\}}} \mathrm{d}\tau
\end{aligned}
\tag{1}
$$

where $\alpha = n - 1 + \{\alpha\}$, $\{\alpha\} \in (0,1)$ and f is assumed to be smooth enough. One should note that this concept of the fractional derivative is equivalent to other well known approach known as *Grünwald-Letnikov* derivative (refer to Theorems 20.2 and 20.4 in [21]).

For a function $f \colon \mathbb{R} \to \mathbb{R}$ whose derivative $f^{(n-1)}$ is bounded on intervals $(-\infty, t)$ and locally Hölder with exponent $\lambda > \{\alpha\}$, the Marchaud derivative of the order α of the function f exists [21, Section 5.4]. It means that the functions $\sin(\omega t)$, $\cos(\omega t)$ and $e^{j\omega t}$ have the Marchaud derivative of any order $\alpha > 0$. Moreover, one obtains the formula (discussed for the Grünwald-Letnikov derivative in [24, Formula (2.65)])

$$
D^\alpha e^{j\omega t} = (j\omega)^\alpha e^{j\omega t}
\tag{2}
$$

allowing us to apply the phasor representation of the electromagnetic field. Furthermore, the Marchaud derivative gives $D^\alpha C = 0$ for any order $\alpha > 0$ and any constant $C \in \mathbb{R}$.

Throughout the paper, we consider functions and vector fields defined for $V \subset \mathbb{R}^3$ being a compact volume with the boundary S being a piecewise smooth surface. It is assumed that all functions $f \colon \mathbb{R} \times V \to \mathbb{R}$ and vector fields $\mathbf{F} \colon \mathbb{R} \times V \to \mathbb{R}^3$ are of an appropriate smoothness for the considered volume V.

III. FO MAXWELL'S EQUATIONS

Let us consider Maxwell's equations in isotropic and homogeneous media

$$
\nabla \cdot \mathbf{D} = \rho
\tag{3}
$$

$$
\nabla \times \mathbf{E} = -\frac{\partial \mathbf{B}}{\partial t}
\tag{4}
$$

$$
\nabla \cdot \mathbf{B} = 0
\tag{5}
$$

$$
\nabla \times \mathbf{H} = \frac{\partial \mathbf{D}}{\partial t} + \mathbf{J}.
\tag{6}
$$

In (3)–(6), $\mathbf{E}$ and $\mathbf{H}$ denote respectively the electric- and magnetic-field intensities, $\mathbf{D}$ and $\mathbf{B}$ denote respectively the displacement- and magnetic-flux densities, $\mathbf{J}$ denotes the current density, ρ denotes the charge density.

Constitutive relations for a medium described by FOM are formulated as follows [10], [11], [18]:

$$
\mathbf{J} = \sigma_\alpha D_t^{1-\alpha} \mathbf{E}, \quad 0 < \alpha \le 1
\tag{7}
$$

$$
\epsilon_\beta \mathbf{E} = D_t^{1-\beta} \mathbf{D}, \quad 0 < \beta \le 1
\tag{8}
$$

$$
\mu_\gamma \mathbf{H} = D_t^{1-\gamma} \mathbf{B}, \quad 0 < \gamma \le 1.
\tag{9}
$$

These equations reduce to the classical constitutive relations of media described by IO model (IOM) for $\alpha = 1$, $\beta = 1$ and $\gamma = 1$. For a vacuum, the conductivity $\sigma_1 = 0$ and the permittivity and permeability are respectively denoted as ϵ_0 and μ_0. The following SI units for the material parameters are taken: $[\sigma_\alpha] = \frac{(\Omega m)^{-1}}{sec^{\alpha-1}}$, $[\epsilon_\beta] = \frac{F}{sec^{1-\beta}m}$, $[\mu_\gamma] = \frac{H}{sec^{1-\gamma}m}$. Let us consider a free space without charge and current sources. Using (7)–(9), one obtains from (3)–(6) the following FO Maxwell's equations in TD:

$$
\nabla \cdot \mathbf{E} = 0
\tag{10}
$$

$$
\nabla \times \mathbf{E} = -\mu_\gamma D_t^\gamma \mathbf{H}
\tag{11}
$$

$$
\nabla \cdot \mathbf{H} = 0
\tag{12}
$$

$$
\nabla \times \mathbf{H} = \epsilon_\beta D_t^\beta \mathbf{E} + \sigma_\alpha D_t^{1-\alpha} \mathbf{E}.
\tag{13}
$$

Let us consider the phasor representation of the electromagnetic field, i.e.

$$
\mathbf{E} = \Re(\tilde{\mathbf{E}} e^{j\omega t})
\tag{14}
$$

$$
\mathbf{H} = \Re(\tilde{\mathbf{H}} e^{j\omega t})
\tag{15}
$$

where $\tilde{\mathbf{E}}$ and $\tilde{\mathbf{H}}$ are electric and magnetic field phasors that are functions of the spatial variables only and ω denotes the angular frequency. From (10)–(15), one obtains FO Maxwell's equations in FD

$$
\nabla \cdot \tilde{\mathbf{E}} = 0
\tag{16}
$$

$$
\nabla \times \tilde{\mathbf{E}} = -\mu_\gamma (j\omega)^\gamma \tilde{\mathbf{H}}
\tag{17}
$$

$$
\nabla \cdot \tilde{\mathbf{H}} = 0
\tag{18}
$$

$$
\nabla \times \tilde{\mathbf{H}} = \epsilon_\beta (j\omega)^\beta \tilde{\mathbf{E}} + \sigma_\alpha (j\omega)^{1-\alpha} \tilde{\mathbf{E}}.
\tag{19}
$$

Hence, the electromagnetic field can be analysed with the use of (16)–(19) in the spatial domain only for a single frequency of an excitation.

IV. SIMULATION ALGORITHMS

The time evolution of the wave propagation can be simulated with the use of TD and FD methods. In this section, two algorithms are presented allowing for the plane-wave simulation in media described by FOM. It is assumed that the diffusive wave propagates along the z direction and the electric- and magnetic-field vectors are along the x and y directions, respectively. For the sake of brevity, we assume that $\sigma_\alpha = 0$. The signalling initial-boundary value condition is considered which describes impinging of the plane wave on the half-space being a medium described by FOM. Then, the wave is transferred into the medium and its TD waveform can be computed as presented below.

A. TD Method

The electric and magnetic fields are given by $\mathbf{E} = E_x\mathbf{i_x} = E(z,t)\mathbf{i_x}$ and $\mathbf{H} = H_y\mathbf{i_y} = H(z,t)\mathbf{i_y}$, respectively. Using the semigroup property of the Marchaud derivative (see [25] and [24, Section 2.6.1] for more detailed explanations resulting from the equivalence to the Grünwald-Letnikov derivative), the following FO diffusion-wave equation for the electric-field intensity can be obtained from (10)–(13) in TD:

$$\epsilon_\beta\mu_\gamma D_t^{\beta+\gamma} E = D_z^2 E. \tag{20}$$

The signalling initial-boundary value condition is formulated for (20) as follows:

$$E(z,0^+) = 0, \qquad z > 0 \tag{21}$$
$$D_t E(z,0^+) = 0, \qquad z > 0 \tag{22}$$
$$E(0^+,t) = h(t), \qquad t > 0 \tag{23}$$
$$E(+\infty,t) = 0, \qquad t > 0. \tag{24}$$

It is further assumed that $\beta + \gamma = 2\nu$ and $\nu \in (0.5, 1)$, i.e., only solutions between the diffusion and the wave propagation are considered. TD Green's function for (20) is given by [19]

$$\mathcal{G}_s(z,t) = \frac{2\nu z}{\pi t} \int_0^\infty E_{2\nu}(-\kappa^2 t^{2\nu}) \cos(x\kappa)\mathrm{d}\kappa \tag{25}$$

when $\epsilon_\beta\mu_\gamma = 1$. In (25), $E_{2\nu}$ denotes the Mittag-Leffler function defined as ($\alpha = 2\nu$)

$$E_\alpha(z) = \sum_{n=0}^{+\infty} \frac{z^n}{\Gamma(\alpha n + 1)} \qquad \alpha > 0, z \in \mathbb{C}. \tag{26}$$

Hence, the solution to the signalling problem (20)–(24) is the convolution of TD Green's function (25) with the excitation signal $h(t)$

$$E(z,t) = \int_0^t \mathcal{G}_s(z, t-\tau)h(\tau)\mathrm{d}\tau. \tag{27}$$

The formula (25) cannot be used directly, as it is derived for the normalized equation (20), i.e., with $\epsilon_\beta\mu_\gamma = 1$. So first, the appropriate change of variables $z \rightarrow \hat{z} = z/L$, $t \rightarrow \hat{t} = t/T$ should be applied, refer to [19] for details.

B. FD Method

The electric and magnetic fields are given by $\tilde{\mathbf{E}} = \tilde{E}_x\mathbf{i_x} = \tilde{E}(z)\mathbf{i_x}$ and $\tilde{\mathbf{H}} = \tilde{H}_y\mathbf{i_y} = \tilde{H}(z)\mathbf{i_y}$, respectively. Then, the following FO diffusion-wave equation for the electric-field intensity can be obtained in FD from (16)–(19):

$$\nabla^2\tilde{E} - \mu_\gamma\epsilon_\beta(j\omega)^{\beta+\gamma}\tilde{E} = 0. \tag{28}$$

Hence, the propagation of diffusive wave can be described in FD for the signalling problem with the use of the transfer function [18]

$$T(\omega) = e^{-\xi(\omega)z} \tag{29}$$

where

$$\xi(\omega) = \frac{\omega^{\frac{\beta+\gamma}{2}}}{c_{\beta\gamma}} e^{j\frac{\pi}{4}(\beta+\gamma)} \tag{30}$$

and

$$c_{\beta\gamma} = \frac{1}{\sqrt{\mu_\gamma\epsilon_\beta}}. \tag{31}$$

The algorithm of the diffusive-wave simulation can be formulated for the excitation $h(t)$ as follows:

- From a real data sequence $h(t)$, calculate the analytic signal $h_a(t) = h(t) + jg(t)$ with the use of the Hilbert transformation ($g(t) = \mathcal{H}[h(t)]$) [20].
- Calculate the Fourier transformation of the analytic signal $h_a(t)$, i.e., $\tilde{H}(\omega) = \mathcal{F}[h_a(t)]$.
- The amplitude of the plane wave at the distance z is calculated as $\tilde{E} = \tilde{H}(\omega)T(\omega)$.
- The TD waveform $E(z,t)$ of the signal at the distance z is the real part of the inverse Fourier transformation of $\tilde{E}$, i.e., $E(z,t) = \Re[\mathcal{F}^{-1}[\tilde{E}]]$.

The first two steps of the algorithm can be combined together because $\mathcal{F}[\mathcal{H}[h(t)]] = -j\mathrm{sgn}(\omega)\mathcal{F}[h(t)]$.

One can avoid computations of the non-elementary TD Green's function with the use of the FD algorithm. However, the applicability of the FD algorithm is limited as far as the orders of time derivatives β, γ are concerned. It stems from the implementation of the method in the discrete-time domain [18]. The multiplier $e^{-\xi z} = e^{-(\Re\xi)z}e^{-j(\Im\xi)z}$ involves the attenuation and the phase delay of the propagating wave. From this point of view, the phase delay must be greater or equal to the phase shift corresponding to the sampling time T_s of the complex signal $h_a(t)$. It gives the condition (see Formula (49) in [18]) for a minimum value of the sum of β and γ coefficients allowing for the application of the FD simulation algorithm, i.e.

$$\frac{z}{c_{\beta\gamma}}\left(\frac{2\pi}{T_s}\right)^{\frac{\beta+\gamma}{2}} \sin\left(\frac{\pi}{4}(\beta+\gamma)\right) \geq 2\pi. \tag{32}$$

V. NUMERICAL RESULTS

Both TD and FD algorithms are implemented in Wolfram Mathematica version 12.0 [26]. The Mittag-Leffler function is computed by means of the built-in function *MittagLefflerE*. A numerical integration is performed on the unbounded domain $(0, +\infty)$ with the method *LocalAdaptive* and the parameter *AccuracyGoal* (AG) set to 6 and 10. The *Fourier* and *InverseFourier* transformations are called with the attribute *FourierParameters* set to $\{1, -1\}$. The computations are performed with the assumption $\epsilon_\beta\mu_\gamma = \epsilon_0\mu_0 = 1/c^2$ (but in $\frac{sec^{\beta+\gamma}}{m^2}$ SI units). The time-step size is set to $\Delta t = 5$ fsec allowing for the application of the FD algorithm (according to Formula (32)). The computations of TD Green's function and a signal propagating in media described by FOM are executed for two distances $L = 1$ mm and $L = 10$ mm of the wave propagation. In the first case, the simulation consists of 1 000 samples whilst, in the second case, the simulation consists of 6 000 samples. The number of samples in the simulation corresponds to the total time of simulation, which is set to 5 psec and 30 psec, respectively. It is verified that the condition (32) is satisfied for the numerical results presented below.
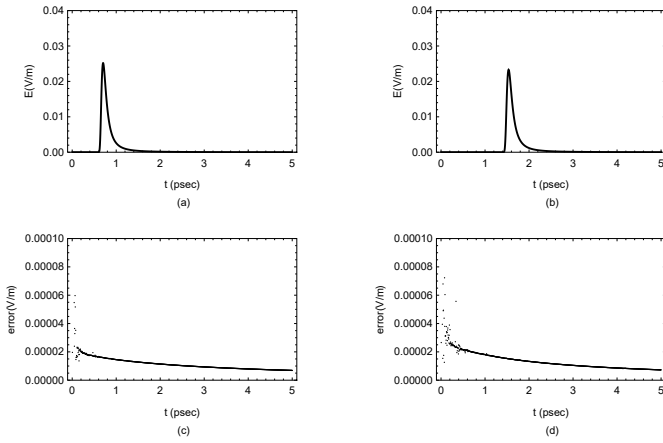
Fig. 1. Green's function at the distance $L = 1$ mm. (a) FD computations for $\nu = 0.95$. (b) FD computations for $\nu = 0.975$. (c) Difference between FD and TD computations for $\nu = 0.95$ and $AG = 10$. (d) Difference between FD and TD computations for $\nu = 0.975$ and $AG = 10$.
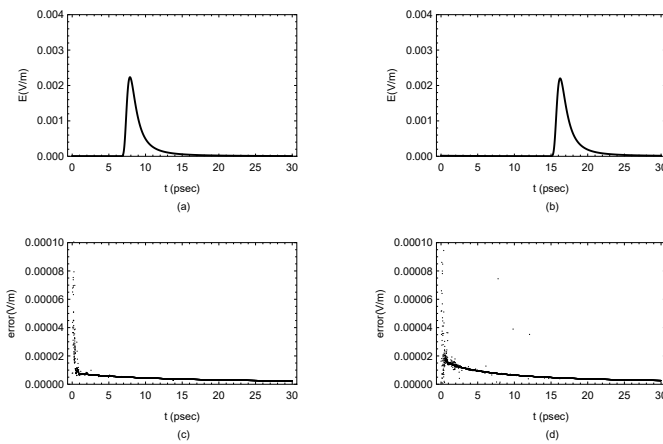

Fig. 2. Green's function at the distance $L = 10$ mm. (a) FD computations for $\nu = 0.95$. (b) FD computations for $\nu = 0.975$. (c) Difference between FD and TD computations for $\nu = 0.95$ and $AG = 10$. (d) Difference between FD and TD computations for $\nu = 0.975$ and $AG = 10$.

A. Accuracy

In Figs. 1 and 2, results of Green's function computations are presented (i.e., $h(t) = \delta(t)$ where δ denotes Dirac's delta function). Because the results of TD and FD computations are visually almost identical, the results of FD computations are presented only in subfigures (a)–(b) with the difference between TD and FD results in subfigures (c)–(d). The TD results are evaluated for two different accuracy parameters ($AG = 6$ and $AG = 10$, results for $AG = 10$ presented in subfigures (c)-(d)), which correspond to substantially different computation times (but almost identical numerical results). One should note that for small values of the time t, TD Green's function computations tend to have large error. It may be explained by the behaviour of the integrated function (25), which for $t \approx 0$ is very close to the cosine function and the integral over $[0, \infty)$ converges very slowly. Hence, the integration method either needs more time steps to converge or

fails to converge at all. For example, for $\nu = 0.975$ and $L = 1$ mm, the maximal error of computations is equal to 0.0185401 (for both $AG = 6$ and $AG = 10$), with the maximal value of the reference function equal to 0.0233052. It is relatively large error (about 80%), but this phenomenon disappears when one moves away from $t = 0$. When one finds the maximal error for samples starting from the sample number 100, the difference drops down to $2 \cdot 10^{-5}$ (which is less than 0.1% of the maximal value of the function). For other values of ν and L, one may observe similar effects. It directly results from assumed integration parameters employed in computations. These examples demonstrate clearly advantages of the FD method which does not suffer from any convergence problems.

Using (27), one can simulate propagation of non-monochromatic waves in media described by FOMs. In Figs. 3 and 4, results of simulations of the propagation of four sinusoidal pulses of the total length 0.5 psec are presented. The frequency of the sinusoidal wave enveloped by the gate function is set to 8 THz. As seen, the signal waveform is significantly distorted, especially when observed in the distance $L = 10$ mm. However, a small perturbation of the time-derivative orders in Maxwell's equations (10)–(13) makes it possible to observe pulses at an observation point earlier than in the case of the linear medium described by IOM (i.e., a vacuum in this test) [18]. Hence, small decrease of the time-derivative orders in Maxwell's equations allows for advancing a signal propagation in an electromagnetic medium.
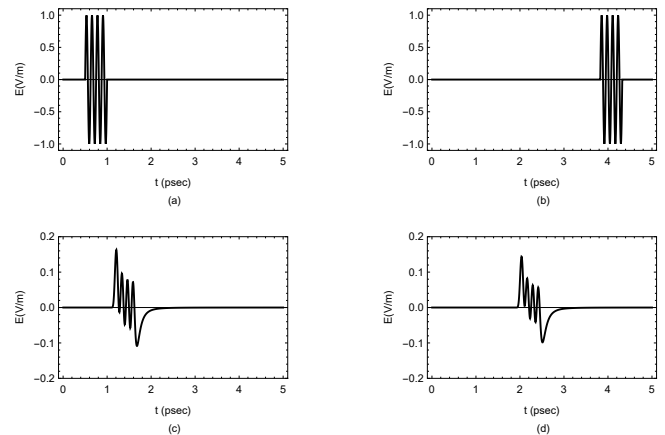

Fig. 3. Response to the sinusoidal pulse excitation at the distance $L = 1$ mm. (a) the sinusoidal pulse. (b) $\nu = 1$ (vacuum). (c) $\nu = 0.95$. (d) $\nu = 0.975$.

B. Computation Times

In general, the time of convolution computations (27) is negligible in comparison with the time of TD Green's function (25) generation for the TD method. Therefore, computation times needed to generate Green's function are only compared in Tab. I. Each numerical experiment is repeated twice to confirm that obtained times do not differ significantly between runs. As seen, computation times of the FD method are negligible in comparison to the TD method times. For $L = 10$ mm, the FD vs. TD speedup approaches 6 orders in magnitude
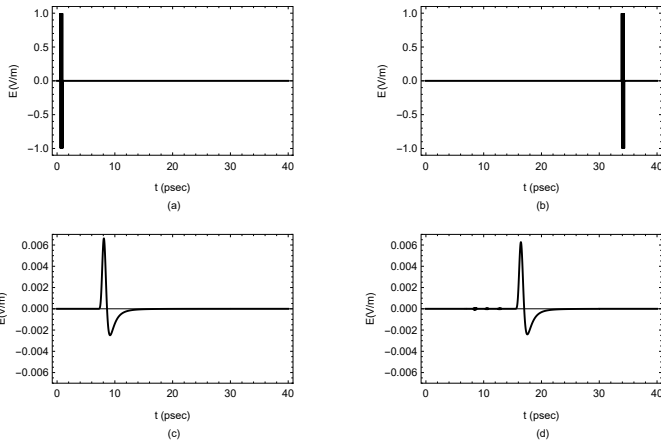
Fig. 4. Response to the sinusoidal pulse excitation at the distance $L = 10$ mm. (a) the sinusoidal pulse. (b) $\nu = 1$ (vacuum). (c) $\nu = 0.95$. (d) $\nu = 0.975$.

TABLE I
COMPUTATION TIMES OF TD GREEN'S FUNCTION

L	ν	TD AG = 6	TD AG = 10	FD
(mm)		(sec)	(sec)	(sec)
1	0.95	5 151	6 812	0
1	0.975	9 639	10 883	0
10	0.95	48 696	51 610	0.04687
10	0.975	92 521	93 974	0.03125

for $AG = 10$ demonstrating advantages of the FD method. The difference results mainly from a long time of the Mittag-Lefler function generation and the integration on unbounded domain in the TD method.

Another interesting observation is that the time needed to compute the value of TD Green's function for points $t \approx 0$ is greater than for larger times t. This observation is demonstrated in Fig. 5.
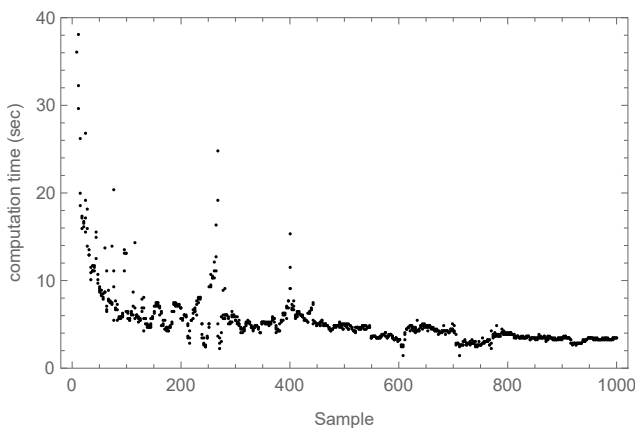

Fig. 5. Computation time for each sample of TD Green's function when $\nu = 0.95$, $AG = 6$, $L = 1$ mm.

VI. CONCLUSION

The wave propagation in electromagnetic media described by FOMs is presented. The algorithms of the non-monochromatic wave simulation are developed which employ computations in TD and FD. Numerical results and computation times obtained with the use of both algorithms are presented and discussed in detail. The FD method significantly outperforms the TD method in terms of accuracy and computation time. However, its applicability is limited by the sampling theorem.

ACKNOWLEDGEMENT

REFERENCES

[1] M. J. Curie, "Recherches sur la conductibilit des corps cristallises," *Annales de chimie et de physique*, vol. 18, pp. 203–269, 1889.
[2] S. Westerlund and L. Ekstam, "Capacitor theory," *IEEE Trans. Dielectr. Electr. Insul.*, vol. 1, no. 5, pp. 826–839, 1994.
[3] J. A. Tenreiro Machado and A. M. S. F. Galhano, "Fractional order inductive phenomena based on the skin effect," *Nonlinear Dyn.*, vol. 68, no. 1, pp. 107–115, 2012.
[4] A. Jalloul, J.-C. Trigeassou, K. Jelassi, and P. Melchior, "Fractional order modeling of rotor skin effect in induction machines," *Nonlinear Dyn.*, vol. 73, no. 1, pp. 801–813, 2013.
[5] V. E. Tarasov, "Fractional vector calculus and fractional Maxwell's equations," *Ann. Phys.*, vol. 323, no. 11, pp. 2756–2778, 2008.
[6] M. D. Ortigueira, M. Rivero, and J. J. Trujillo, "From a generalised Helmholtz decomposition theorem to fractional Maxwell equations," *Comm. Nonlinear Sci. Numer. Simulat.*, vol. 22, no. 1, pp. 1036–1049, 2015.
[7] E. K. Jaradat, R. S. Hijjawi, and J. M. Khalifeh, "Maxwell's equations and electromagnetic Lagrangian density in fractional form," *J. Math. Phys.*, vol. 53, no. 3, p. 033505, 2012.
[8] H. Nasrolahpour, "A note on fractional electrodynamics," *Comm. Nonlinear Sci. Numer. Simulat.*, vol. 18, no. 9, pp. 2589–2593, 2013.
[9] D. Baleanu, A. K. Golmankhaneh, A. K. Golmankhaneh, and M. C. Baleanu, "Fractional electromagnetic equations using fractional forms," *Int. J. Theor. Phys.*, vol. 48, no. 11, pp. 3114–3123, 2009.
[10] M. A. Moreles and R. Lainez, "Mathematical modelling of fractional order circuit elements and bioimpedance applications," *Comm. Nonlinear Sci. Numer. Simulat.*, vol. 46, pp. 81–88, 2017.
[11] T. P. Stefanski and J. Gulgowski, "Electromagnetic-based derivation of fractional-order circuit theory," *Comm. Nonlinear Sci. Numer. Simulat.*, vol. 79, p. 104897, 2019.
[12] R. Ismail and A. G. Radwan, "Rectangular waveguides in the fractional-order domain," in *2012 International Conference on Engineering and Technology (ICET)*, Oct 2012, pp. 1–6.
[13] S. M. Cvetićanin, D. Zorica, and M. R. Rapaić, "Generalized time-fractional telegrapher's equation in transmission line modeling," *Nonlinear Dyn.*, vol. 88, no. 2, pp. 1453–1472, 2017.
[14] N. A.-Z. R-Smith, A. Kartci, and L. Brank, "Application of numerical inverse Laplace transform methods for simulation of distributed systems with fractional-order elements," *J. Circuits Syst. Comput.*, vol. 27, no. 11, p. 1850172, 2018.
[15] A. Shamim, A. G. Radwan, and K. N. Salama, "Fractional Smith chart theory," *IEEE Microw. Wireless Compon. Lett.*, vol. 21, no. 3, pp. 117–119, 2011.
[16] Y. Shang, W. Fei, and H. Yu, "A fractional-order RLGC model for tera-hertz transmission line," in *2013 IEEE MTT-S International Microwave Symposium Digest (MTT)*, June 2013, pp. 1–3.
[17] Y. Shang, H. Yu, and W. Fei, "Design and analysis of CMOS-based ter-ahertz integrated circuits by causal fractional-order RLGC transmission line model," *IEEE Trans. Emerg. Sel. Topics Circuits Syst.*, vol. 3, no. 3, pp. 355–366, Sep. 2013.
[18] T. P. Stefanski and J. Gulgowski, "Signal propagation in electromagnetic media described by fractional-order models," *Comm. Nonlinear Sci. Numer. Simulat.*, vol. 82, p. 105029, 2020.

[19] ——, "Fundamental properties of solutions to fractional-order Maxwell's equations," 2020, submitted for publication.

[20] A. V. Oppenheim and R. W. Schafer, *Discrete-Time Signal Processing*, 3rd ed. Upper Saddle River, NJ, USA: Prentice Hall Press, 2009.

[21] S. G. Samko, A. A. Kilbas, and O. I. Marichev, *Fractional Integrals and Derivatives: Theory and Applications*. Gordon and Breach, New York, 1993.

[22] C. Li and F. Zeng, *Numerical Methods for Fractional Calculus*. Chapman and Hall/CRC, 2015.

[23] F. Ferrari, "Weyl and Marchaud derivatives: a forgotten history," *Mathematics*, vol. 6, no. 6, 2018. [Online]. Available: https://www.mdpi.com/2227-7390/6/1/6

[24] M. D. Ortigueira, *Fractional Calculus for Scientists and Engineers*. Berlin, Heidelberg: Lecture Notes in Electrical Engineering, Springer, 2011.

[25] M. D. Ortigueira and J. Tenreiro Machado, "What is a fractional derivative?" *J. Comput. Phys.*, vol. 293, no. C, pp. 4–13, 2015.

[26] Wolfram Research Inc, *Mathematica, Version 12.0*, Champaign, IL, 2019.